EUROPEAN JOURNAL OF MATERIALS SCIENCE AND ENGINEERING
Volume 8, Issue 4, 2023: 249-256 | www.ejmse.ro | ISSN: 2537-4338

EJMSE

DOI: 10.36868/ejmse.2023.08.04.249

INVESTIGATING THE IMPACT OF ANNEALING TEMPERATURE ON THE MICROSTRUCTURE AND MECHANICAL PERFORMANCE OF SELECTIVELY LASER MELTED Ti6Al4V ALLOY

Hassanen JABER[1], János KÓNYA[2], Péter PINKE[1], László TÓTH[1], Tünde Anna KOVÁCS[1*]

[1]Óbuda University, Bánki Donát Faculty of Mechanical and Safety Engineering,
Népszínház str. 8 1081 Budapest, Hungary
[2]Óbuda University, Doctoral School on Materials Sciences and Technologies, Bécsi str. 96/B 1034 Budapest, Hungary

Abstract

This research addresses the metallurgical and mechanical response during the annealing of Ti6Al4V parts fabricated by selective laser melting. The as-manufactured Ti6Al4V exhibited a very fine α´ martensitic structure with low ductility of less than 10%. It was observed that the fine α´ martensitic structure transformed into two phases of α and β by applying heat treatments at 850 and 1020 °C followed by furnace cooling. The experimental results demonstrated that 850°C/2h/FC heat treatment has optimum mechanical performance in terms of tensile strength and ductility.

Keywords*: Selective Laser Melting (SLM), Ti6Al4V, annealing, additive technology*

Introduction

Owing to their high biocompatibility, low ion release, high corrosion resistance, and high mechanical properties, Ti6Al4V alloy plays a main factor in the automotive, aerospace, and biomedical industries [1-4].

Selective laser melting (SLM) is a common kind of 3D printing (additive manufacturing) in the biomedical, aerospace, and automotive industries due to the design freedom of complex shapes, high precision, cost savings, and production speed [5-8].

SLM is a 3D printing fusion technology in which heat is produced by the ability of the powder material being bonded to absorb energy from a focused laser beam [9]. During the SLM, the powder material is subjected to high temperatures and melted beyond its melting point [10]. The molten material is then allowed to cool rapidly and solidify into the desired shape. A major flaw of Ti6Al4V parts produced by SLM is the low ductility of less than 10% [11, 12]. The low ductility of the SLMed Ti6Al4V alloy results from the formation of a very fine α´ martensitic structure [13]. The α´ martensitic phase is a vanadium-rich, supersaturated substitutional solid solution in a close-packed hexagonal structure [14], which was formed in the SLMed Ti6Al4V parts as an outcome of the high cooling rate ac-companied with the SLM system. The formation of the α´ martensitic phase is associated with the presence of residual stresses [14], which ultimately lead to a loss of ductility.

Therefore, in this paper, the effects of annealing at 850 and 1020 ºC on the microstructure-properties relationship of annealed Ti6Al4V alloy produced by SLM are examined.

*Corresponding author: kovacs.tunde@bgk.uni-obuda.hu

Materials and Experiments

Gas-atomized spherical Ti6Al4V powder (Fig. 1), which has a nominal particle size ranging from 15 to 45 µm, was employed as the primary material. Its chemical composition is demonstrated in Table 1. The samples of the tensile test are manufactured on a Sisma Mysint 100 machine, which includes a laser unit delivering a continuous laser power of 200 W. The laser power, layer thickness, and scan speed were all maintained at the same level, as illustrated in Table 2. At a flow rate of 34 liters per minute, pure argon gas was employed as a shield. Tensile test specimens were manufactured using the dimensions given in Fig. 1.

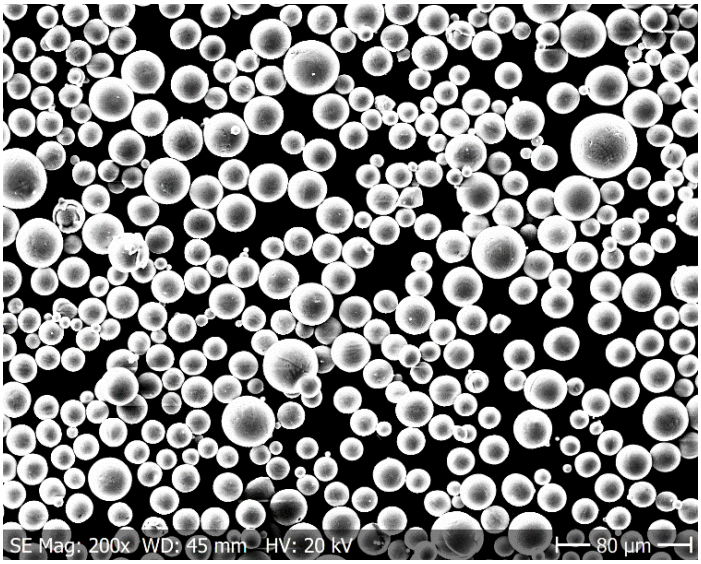

Fig. 1. SEM microscopic image showing the morphology of Ti6Al4V alloy powder

The chemical composition of the Ti64 powder with ASTM specification (Table 1).

Table 1. Chemical compositions (wt %) of the investigated Ti64 powder with ASTM specification

Mass%		Al	V	Fe	O	N	C	H	Ti
Ti6Al4V powder		6.11	4.02	0.17	0.090	0.023	0.01	0.003	Bal.
ASTM	Max	6.50	4.50	0.25	0.13	0.03	0.08	0.0125	Bal.
B348 Gr.23	Min	5.50	3.50						Bal.

The used SLM process parameters as laser power, scan speed, layer thickness and hatch spacing are summarized in Table 2.

Table 2. SLM parameters used in the manufacturing of Ti6Al4V parts

Laser power	125 W
scan speed	1000 mm/s
Layer thickness	20 µm
Hatch spacing	80 µm

The printed test samples were the tensile specimens with the sizes on the Fig. 2.

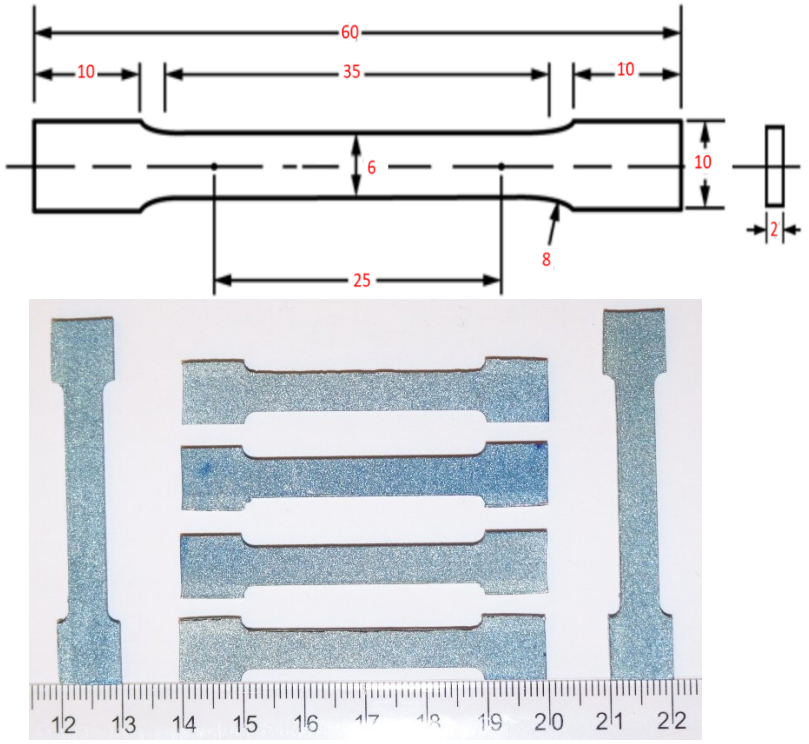

Fig. 2. Dimensions of the manufactured Ti6Al4V tensile samples

After production, two distinct heat treatments were carried out, as indicated in Fig. 3 schematically. The untreated and heat-treated specimens underwent a tensile test at room temperature adopting an Inspekt Retrofit testing machine and testing equipment with a crosshead speed of 1 mm/min in compliance with ASTM E8M [12]. Using Leitz-Wetzlar testing equipment, a Vickers microhardness test was undertaken with a force of 0.5 kgf and a holding time of 10 s. X-ray diffraction and optical microscopy were used to analyze the metallurgical properties of the SLM-produced Ti6Al4V components. The metallographic samples were prepared using the procedure of standard titanium alloy. The microstructure of the specimens was investigated using Kroll's No. 192 etchant [14].

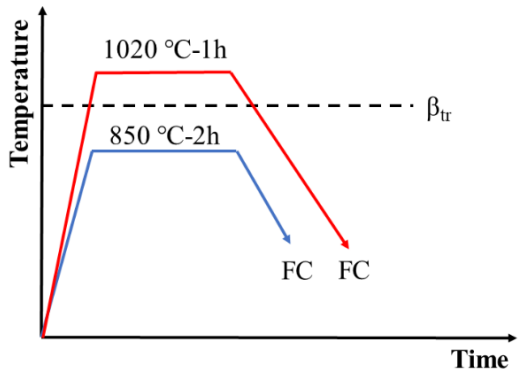

Fig. 3. Heat Treatment cycle

Results and Discussion

Fig. 4 depicts the XRD of the as-processed sample, revealing the presence of close-packed hexagonal peaks associated with α′ martensitic structure. Fig. 5 presents an optical micrograph showing the α′ martensitic structure of the as-processed part for the top view. It is seen that there is a lath morphology and micro-voids. The micro-structure of as-processed can be seen in the high magnification light microscope images from the top and from the side (Fig. 6 A, B). The morphology of the microstructures is not uniform. Recrystallization during SLM is responsible for the observation of equiaxed grains of β phase with a diameter of approximately 74 μm, completely interspersed with α′ martensite (Fig. 6A, top view). In contrast to what can be seen from the side, this is something completely new (Fig. 6B). In the side view of morphology, columnar β grains can be seen forming epitaxially as the material melts and resolidifies between each layer deposit. The hatch spacing chosen to produce the samples results in columnar grains about 78 μm wide.

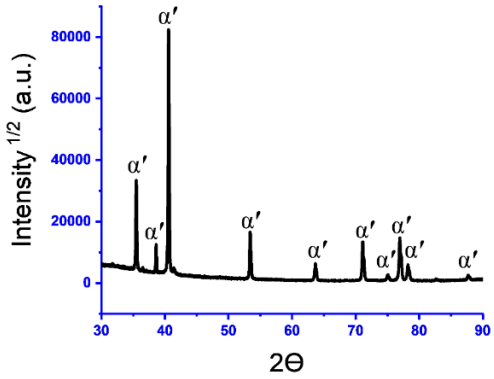

Fig. 4. XRD of as-processed Ti6Al4V

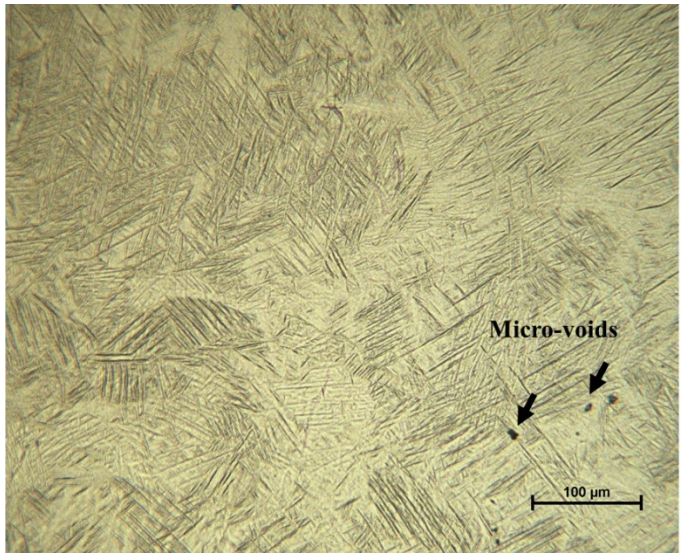

Fig. 5. Optical micrograph proving α′ martensitic phase of the as-processed Ti6Al4V

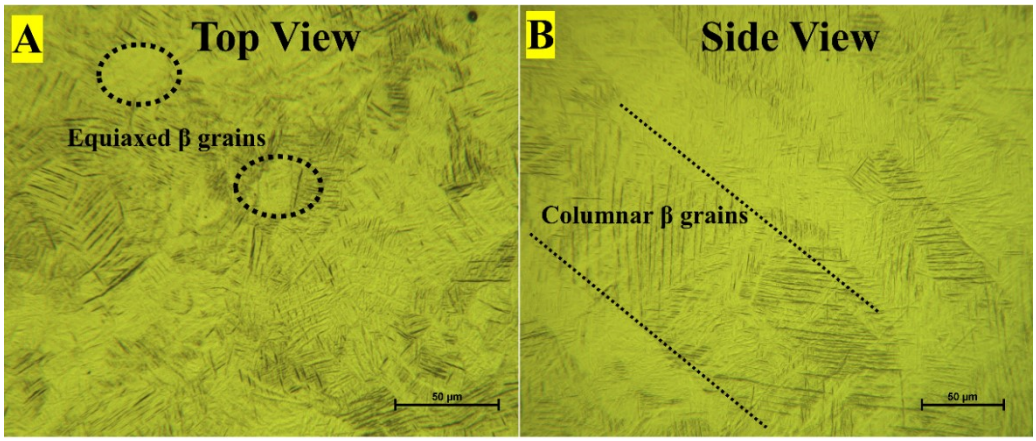

Fig. 6. (A) An optical image showing the top view of as-processed Ti6Al4V, revealing fully martensite equiaxed grain morphologies. (B) A side view optical micrograph of as-processed Ti6Al4V, revealing the material's characteristic columnar grains

Fig. 7 and 8 show the X-ray diffraction of the 850 °C/FC and 1020 °C/FC heat treated samples respectively, identifying a dual-phase crystalline structure consisting of α phase (close-packed hexagonal) and β phase (body-centered cubic). The planes at (110) and (211) are related to the β phase. Fig. 9 illustrates the microstructure of the 850 °C/FC heat-treated part. The microstructure is composed of 25.4% β phase and 74.6 α. Fig. 10 shows the microstructure of the Ti6Al4V after 1020 °C/FC heat treatment. The microstructure is composed of 29.7% β phase and 70.3 α.

Fig. 11 compares the hardness results of the untreated and heat-treated samples with both heat-treatment temperatures 850 and 1020 °C. As-processed Ti6Al4V has a hardness of ~377 HV. The hardness of the samples that were heat treated was found to be lower than the hardness of the as-processed condition. The presence of the α′ martensitic phase is known to cause the greater hardness of Ti6Al4V in as-processed conditions.

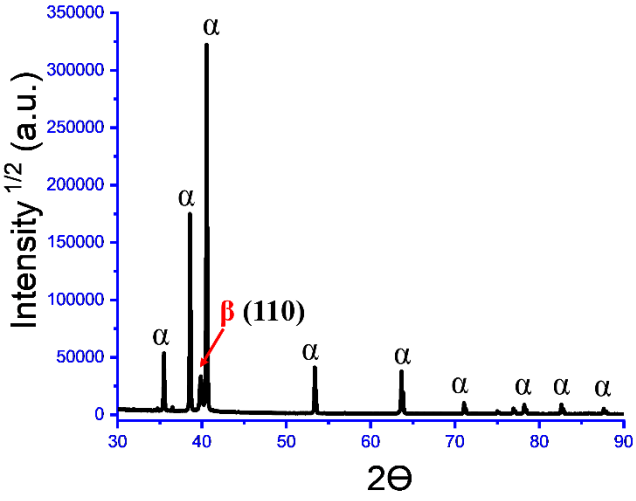

Fig. 7. The x-ray diffraction result of the SLMed Ti6Al4V samples heat treated at 850 °C/FC

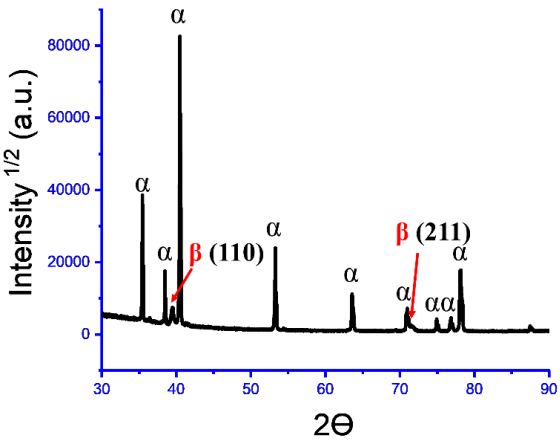

Fig. 8. The x-ray diffraction result of the SLMed Ti6Al4V samples heat treated at 1020 °C/FC

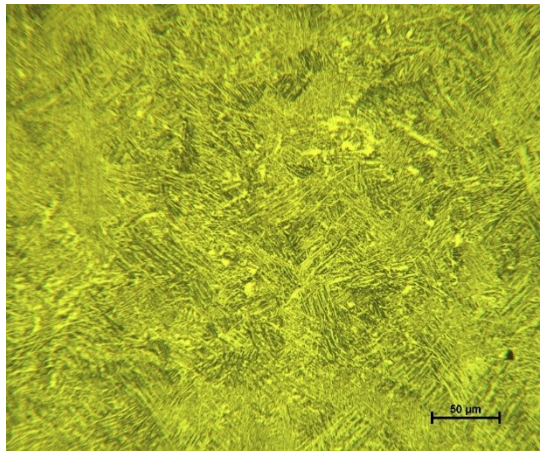

Fig. 9. Optical micrograph showing α and β structure of 850 °C/FC heat treated Ti6Al4V

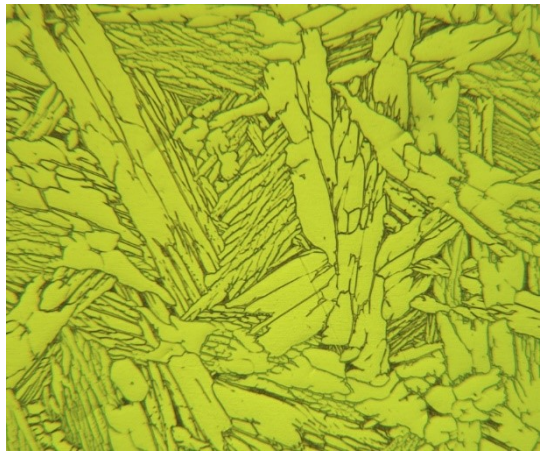

Fig. 10. Optical micrograph showing α and β structure of 1020 °C/FC heat treated Ti6Al4V

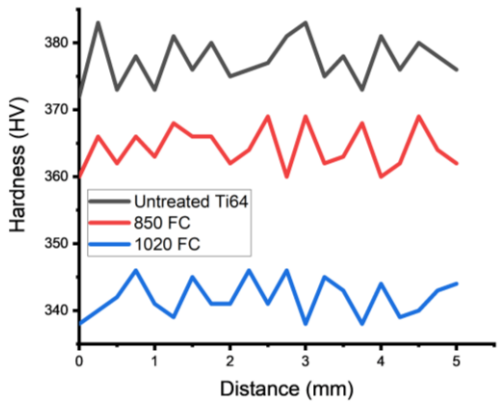

Fig. 11. A typical hardness profile of the untreated and heat-treated Ti6Al4V specimens

To explore the mechanical performance of the SLM components in the untreated condition and after different heat treatments, a tensile test was carried out. Fig. 12 compares and summarizes the tensile test results on the untreated condition with those of after heat treatments. As can be seen, heat treatments lowered strength and increased elongation. It's worth noting that the heat treatment at 850°C/2h/FC yields the finest possible mix of ductility and strength.

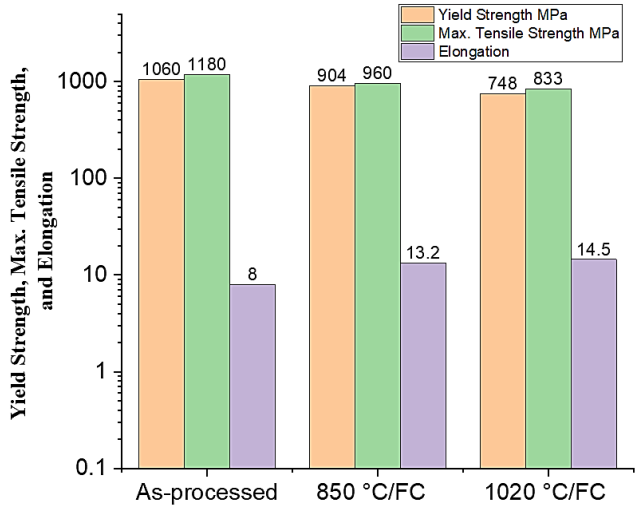

Fig. 12. Tensile properties of the untreated condition and after various heat treatments

Conclusions

The extremely high cooling rate (104 $K \cdot s^{-1}$) combined with SLM resulted in the Ti-6Al-4V components acquiring a very fine α′ martensitic structure. By applying heat treatments at 850 and 1020 °C followed by furnace cooling, the transformation of a fine crystalline α′ martensitic structure into a two-phase microstructure consisting of α and β was observed. This was accompanied by increased ductility and decreased strength. However, the heat treatment at 850°C/2h/FC yields the finest possible mix of ductility and strength.

References

[1] H. Jaber and T. Kovacs, *Selective laser melting of Ti alloys and hydroxyapatite for tissue engineering: progress and challenges*, **Mater. Res. Express**, **6(8)**, 2019, p. 082003. doi: 10.1088/2053-1591/ab1dee.

[2] H. Jaber, J. Kónya, and T. A. Kovács, *Selective laser melting of ti6al4v-2%hydroxyapatite composites: Manufacturing behavior and microstructure evolution*, **Metals (Basel)**, 11(8), 2021, pp. 1–15. doi: 10.3390/met11081295.

[3] M.S. Baltatu, C. Chirac-Moruzzi, P. Vizureanu, L. Tóth and J. Novák, *Effect of Heat Treatment on Some Titanium Alloys Used as Biomaterials*, **Applied Science**, **12**, 2022, p. 11241. doi: 10.3390/app12211124.

[4] M.-C. Spataru, F.D. Cojocaru, A.V. Sandu, C. Solcan, I.A. Duceac, M.S. Baltatu, I. Voiculescu, V. Geanta, P. Vizureanu, *Assessment of the Effects of Si Addition to a New TiMoZrTa System,* **Materials**, **14**, 2021, p. 7610. doi: 10.3390/ma14247610.

[5] M.S. Bălţatu, P. Vizureanu, P. V. Goanţă, C.A. Ţugui, I. Voiculescu, *Mechanical Tests for Ti-Based Alloys as New Medical Materials,* **IOP Publishing: Bristol**, UK, 2019; Volume 572, p. 012029.

[6] C. Jimenez-Marcos, J.C. Mirza-Rosca, M.S. Baltatu, P. Vizureanu, *Experimental Research on New Developed Titanium Alloys for Biomedical Applications,* **Bioengineering, 9**, 2022, p. 686. doi: 10.3390/bioengineering9110686.

[7] W. E. Frazier, *Metal additive manufacturing: A review*, **J. Mater. Eng. Perform.**, **23(6)**, 2014, pp. 1917–1928. doi: 10.1007/s11665-014-0958-z.

[8] W. S. W. Harun, M. S. I. N. Kamariah, N. Muhamad, S. A. C. Ghani, F. Ahmad, and Z. Mohamed, *A review of powder additive manufacturing processes for metallic biomaterials,* **Powder Technol**, **327**(December), 2018, pp. 128–151. doi: 10.1016/j.powtec.2017.12.058.

[9] H. Jaber, T. Kovacs, and K. János, *Investigating the impact of a selective laser melting process on Ti6Al4V alloy hybrid powders with spherical and irregular shapes*, **Adv. Mater. Process. Technol.**, 2020, doi: 10.1080/2374068X.2020.1829960.

[10] C. Y. Yap et al., *Review of selective laser melting: Materials and applications*, **Appl. Phys. Rev.**, **2(4)**, 2015, pp. 1–22. doi: 10.1063/1.4935926.

[11] H. Jaber, J. Kónya, K. Kulcsár, and T. Kovács, *Effects of Annealing and Solution Treatments on the Microstructure and Mechanical Properties of Ti6Al4V Manufactured by Selective Laser Melting*, **Materials (Basel)**, **15(5)**, 2022, pp. 1–22. doi: 10.3390/ma15051978.

[12] H. Shipley et al., *Optimisation of process parameters to address fundamental challenges during selective laser melting of Ti-6Al-4V : A review*, **Int. J. Mach. Tools Manuf.**, **128**(January), 2018, pp. 1–20. doi: 10.1016/j.ijmachtools.2018.01.003.

[13] L. Facchini et al., *Ductility of a Ti-6Al-4V alloy produced by selective laser melting of pre-alloyed powders*, **Rapid Prototype. J.**, 16(6), 2011, pp. 450–459. doi: 10.1108/13552541011083371.

[14] M. Motyka, K. Kubiak, J. Sieniawski, and W. Ziaja, *Phase Transformations and Characterization of α + β Titanium Alloys*, **Comprehensive Materials Processing**, **2**, 2014, pp. 7–36.

Received: September 29, 2023
Accepted: October 27, 2023